Theoretical model for superluminal and slow light in erbium-doped optical fibers: enhancement of the frequency response by pump modulation

S. Jarabo · A. Schweinsberg · N.N. Lepshkin · M.S. Bigelow · R.W. Boyd

Abstract Superluminal and slow-light propagation in erbium-doped optical fibers are theoretically modeled. The pump and signal fields are allowed to be intensity modulated at the same frequency, and propagation effects are included in the model. The levels of advancement, delay, and distortion are determined as functions of system parameters such as modulation frequency, input pump power, modulation indexes of the pump and signal powers, input signal power, fiber length, and the relative phase of the pump and signal modulation. Two methods are analyzed for enhancing the frequency response while ensuring that distortion values remain tolerable. The first method assumes no modulation of the pump wave, although the pump power is adjusted for each signal modulation frequency. A flat frequency response for frequencies up to several kilohertz is obtained, although signal advancements are limited to low values. In the second method, the pump power is modulated with a phase that needs to be controlled with respect to that of the signal. Advancements and delays are increased by this procedure, and distortion values remain tolerable. The frequency response is not made worse for advancements and it is improved for delays. Moreover, absorption need not accompany slow light for this method.

S. Jarabo (✉)
Departamento de Física Aplicada, Facultad de Ciencias, Universidad de Zaragoza, Pedro Cerbuna, 12, 50009 Zaragoza, Spain
e-mail: sjarabo@unizar.es
Fax: +34-976-761233

A. Schweinsberg · R.W. Boyd
The Institute of Optics, University of Rochester, Rochester, NY 14627, USA

N.N. Lepshkin
San Francisco State University, San Francisco, CA 94132, USA

M.S. Bigelow
St. Cloud State University, St. Cloud, MN 56301, USA

R.W. Boyd
Department of Physics, University of Ottawa, Ottawa, Ontario, Canada

1 Introduction

Superluminal and slow-light propagation are two very interesting phenomena that have been observed and measured in various material systems [1–19]. Moreover, from an applications perspective, the active control of the group velocity of light can be a key issue in the development of new technologies for optical communications, such as optical buffers for all-optical routing, optical memories, and optical signal processing [20–27]. In addition, other new applications are emerging in image processing [28] and interferometry [29, 30].

Since they offer very long interaction lengths and extremely high optical intensities, optical fibers offer a very effective material for all-optical control of the group velocity. Specifically, superluminal and slow-light propagation with long delays and advancements have been experimentally demonstrated in erbium-doped optical fibers [14, 31–37]. These experiments have shown that it is possible to actively control the group velocity by varying the input pump power. Recently, it has been experimentally demonstrated [38] that the group velocity can be also controlled by pump modulation. Nevertheless, although a signal waveform can be easily advanced or delayed by employing erbium-doped fibers, this waveform will always show some level of distortion [14]. As signal distortion is a key concern in many applications,

it is necessary to obtain procedures to control signal advancements/delays while keeping distortion levels tolerable [35, 39].

Although it is possible to study and analyze slow and superluminal propagation at a purely experimental level, it is nonetheless important to develop accurate theoretical models that allow one to predict physical effects, optimize and analyze new experiments, and design applications. In Ref. [14], the authors earlier presented a theoretical explanation of slow- and fast-light effects based on some previous work [31, 33, 38] on the amplification of modulated signals in erbium-doped fibers. Nevertheless, these predictions can be improved by taking into account a more accurate analytic model that included propagation effects for the pump and signal waves [40]; experimental verification of this model has been presented in the literature [41, 42].

In this paper, superluminal and slow-light propagation in erbium-doped optical fibers is analyzed by a simple and accurate theoretical model that allows for modulation of the pump and signal power. Pump and signal distortions can also be determined through use of this model. Furthermore, it can be employed to analyze optimization procedures of advancements and delays of a modulated signal power while keeping a tolerable level of signal distortion. To ensure reliable results, we verify the parameters of our model by fitting our numerical results to the values reported in the measurements of Ref. [14].

2 Theoretical model

We assume that the erbium ions are described by the energy-level scheme shown in Fig. 1, and that light fields created by amplified spontaneous emission do not influence the level populations. Erbium ions are pumped at a rate W_p from ground state up to level 3. From this level, erbium ions decay essentially instantaneously to the upper level of the laser transition, and therefore level 3 can be considered to be empty. The relative populations of the ground and excited levels (n_1 and n_2 respectively) can be determined by means of rate equations taking into account the absorption, stimulated emission, and spontaneous emission rates (W_a, W_e and $A_{21} = 1/\tau$, respectively, τ being the lifetime of the laser transition). The pump and signal rates depend on the pump and signal powers within the erbium-doped fiber (EDF), as also shown in Fig. 1. The pump power is denoted by P_p. The signal power can be either forward propagating or backward propagating and it is denoted by P_s^+ or P_s^-, respectively. Therefore, the level populations can be determined in terms of the pump and signal powers. It is well known [40–42] that these powers evolve along the fiber in accordance with the equations

$$\frac{1}{P_p(z,t)} \frac{\partial P_p(z,t)}{\partial z} = -\gamma_p n_1(z,t), \tag{1}$$
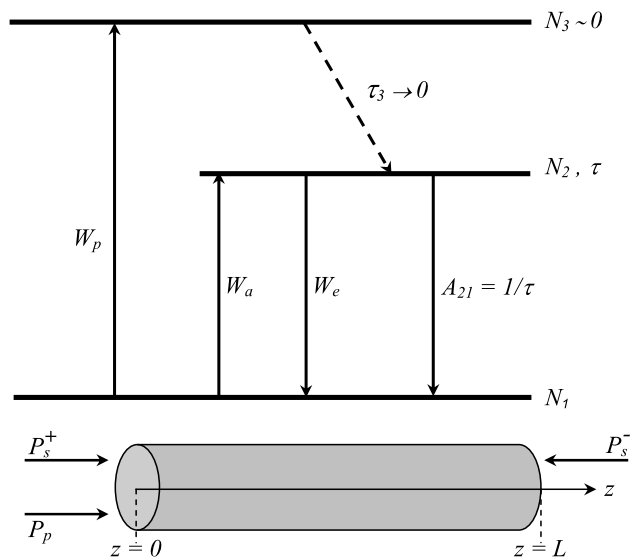
Fig. 1 Energy-level scheme for EDF amplifiers: W_p = pump rate, W_a = absorption rate, W_e = stimulated emission rate, τ = erbium-ion lifetime, P_p = pump power, $P_s^\pm$ = forward and backward propagating signal powers, L = EDF length

$$\frac{1}{P_s^\pm(z,t)} \frac{\partial P_s^\pm(z,t)}{\partial z} = \pm[\gamma_e - (\gamma_a + \gamma_e)n_1(z,t)]$$
$$= \pm g(z,t), \tag{2}$$

where γ_p is the absorption coefficient at the pump wavelength, γ_a and γ_e are absorption and stimulated emission coefficients at the signal wavelength, and $g(z,t)$ is the gain coefficient. These equations illustrate that, when the signal power is modulated, it induces a modulation of populations and, therefore, of the pump power as well, even if the injected pump power does not initially depend on time.

We assume now that the pump and signal powers are weakly modulated as cosine functions according to

$$P_s^\pm(z,t) = P_s^\pm(z)\{1 + r_s^\pm(z)\cos[\omega_m t + \varphi_s^\pm(z)]\}, \tag{3}$$
$$P_p(z,t) = P_p(z)\{1 + r_p(z)\cos[\omega_m t + \varphi_p(z)]\}, \tag{4}$$

where ω_m is the modulation frequency and small modulation indexes are assumed ($r_s^\pm(z) \ll 1$ and $r_p(z) \ll 1$) so that perturbations only up to the first order need be considered. Although notation "$\pm$" is maintained, we assume that the signal power is either forward or backward propagating (but not both simultaneously). Finally, as the populations must also be modulated, we assume that

$$n_1(z,t) = n_1(z)\{1 + r_n(z)\cos[\omega_m t + \varphi_n(z)]\}, \tag{5}$$

with $r_n(z) \ll 1$, and $n_1(z)$ being the steady-state relative population of the ground energy-level, which can be ex-

pressed as

$$n_1(z) = \frac{W_e(z) + A_{21}}{\omega_c(z)} = \frac{1 + \frac{\gamma_e}{\gamma_p} \frac{v_p}{v_s} \frac{P_s^{\pm}(z)}{P_p^{\text{th}}}}{1 + \frac{P_p(z)}{P_p^{\text{th}}} + \frac{\gamma_a + \gamma_e}{\gamma_p} \frac{v_p}{v_s} \frac{P_s^{\pm}(z)}{P_p^{\text{th}}}}, \qquad (6)$$

with

$$\omega_c(z) = W_p(z) + W_a(z) + W_e(z) + A_{21}$$
$$= \frac{1}{\tau} \left[1 + \frac{P_p(z)}{P_p^{\text{th}}} + \frac{\gamma_a + \gamma_e}{\gamma_p} \frac{v_p}{v_s} \frac{P_s^{\pm}(z)}{P_p^{\text{th}}} \right], \qquad (7)$$

and

$$P_p^{\text{th}} = \frac{h v_p}{\tau} \frac{A_d N_T}{\gamma_p}, \qquad (8)$$

since the temporal evolution of the relative population of the ground level can be expressed as

$$\frac{\partial n_1(z,t)}{\partial t} = \left[W_e(z,t) + A_{21} \right] - \left[W_p(z,t) + W_a(z,t) \right.$$
$$\left. + W_e(z,t) + A_{21} \right] n_1(z,t). \qquad (9)$$

Although it is not a precise definition, the quantity P_p^{th} is usually considered to be the threshold pump power of the amplifier, that is, it gives the minimum value of the pump power that must be applied to produce amplification.

Defining the complex functions

$$\xi_q(z) = r_q(z) \exp[i \varphi_q(z)], \quad q = p, n, \qquad (10)$$

substituting Eqs. (4) and (5) into Eq. (1), and neglecting second-order terms, we find that

$$\frac{d \xi_p(z)}{dz} = -\gamma_p n_1(z) \xi_n(z). \qquad (11)$$

In the same way, substituting now Eqs. (3) and (5) into Eq. (2) and neglecting second-order terms again, we find that

$$\frac{d \xi_s^{\pm}(z)}{dz} = \mp (\gamma_a + \gamma_e) n_1(z) \xi_n(z), \qquad (12)$$

with

$$\xi_s^{\pm}(z) = r_s^{\pm}(z) \exp[i \varphi_s^{\pm}(z)]. \qquad (13)$$

Comparing Eqs. (11) and (12), we see that the derivatives are related by

$$\frac{d \xi_p(z)}{dz} = \pm \frac{1}{\beta} \frac{d \xi_s^{\pm}(z)}{dz}, \quad \beta = \frac{\gamma_a + \gamma_e}{\gamma_p}. \qquad (14)$$

Then, by integrating this equation from 0 to z if the signal power is forward propagating or from z to L (EDF length)

if the signal power is backward propagating, one finds that $\xi_s^{\pm}(z)$ and $\xi_p(z)$ are related by

$$\xi_s^{+}(z) - \xi_s^{+}(0) = \beta [\xi_p(z) - \xi_p(0)], \qquad (15)$$
$$\xi_s^{-}(z) - \xi_s^{-}(L) = -\beta [\xi_p(z) - \xi_p(L)]. \qquad (16)$$

On the other hand, $\partial n_1(z,t)/\partial t$ can be obtained by differentiation of Eq. (5) or by means of substituting Eqs. (3), (4), and (5) into Eq. (9) and neglecting second-order terms. Therefore, equating both expressions and taking into account Eqs. (1), (2), (11), and (7), it is obtained that

$$\xi_n(z) = \frac{1}{\gamma_p n_1(z)} \frac{\omega_c(z) - i \omega_m}{\omega_c^2(z) + \omega_m^2}$$
$$\times \left[\frac{d \omega_p(z)}{dz} \xi_p(z) \pm \frac{1}{\beta} \frac{d \omega_s(z)}{dz} \xi_s^{\pm}(z) \right], \qquad (17)$$

provided that the signal power is either forward or backward propagating, and where

$$\omega_p(z) = \frac{1}{\tau} \frac{P_p(z)}{P_p^{\text{th}}} \quad \text{and} \quad \omega_s(z) = \frac{v_p}{v_s} \frac{\beta}{\tau} \frac{P_s^{\pm}(z)}{P_p^{\text{th}}}. \qquad (18)$$

Finally, by substituting Eq. (17) into Eq. (12), we find that

$$\frac{d \xi_s^{\pm}(z)}{dz} = -\frac{\omega_c(z) - i \omega_m}{\omega_c^2(z) + \omega_m^2}$$
$$\times \left[\frac{d \omega_s(z)}{dz} \xi_s^{\pm}(z) \pm \beta \frac{d \omega_p(z)}{dz} \xi_p(z) \right]. \qquad (19)$$

Thus, $\xi_s^{\pm}(z)$ and $\xi_p(z)$ can be determined by solving Eqs. (15), (16), and (19). Therefore, $r_p(z)$, $r_s^{\pm}(z)$, $\varphi_p(z)$, and $\varphi_s^{\pm}(z)$ can be known according to Eqs. (10) and (13). This set of equations is in agreement with, and generalizes results reported by, other authors [31, 33]. However, to solve them, it is necessary to know $P_p(z)$ and $P_s^{\pm}(z)$ in order to determine their derivatives (Eqs. (1), (2), and (6)), and $\omega_c(z), \omega_p(z), \omega_s(z)$ (Eqs. (7) and (18)) and their derivatives.

The pump and signal powers along the fiber can be determined by solving the following set of equations:

$$\gamma_p z + \ln \left[\frac{P_p(z)}{P_p(0)} \right] + \frac{P_p(z) - P_p(0)}{P_p^{\text{th}}}$$
$$+ \frac{v_p}{v_s} \frac{P_s^{+}(0)}{P_p^{\text{th}}} [G(z) - 1] = 0, \qquad (20)$$

$$\gamma_p z + \ln \left[\frac{P_p(z)}{P_p(0)} \right] + \frac{P_p(z) - P_p(0)}{P_p^{\text{th}}}$$
$$+ \frac{v_p}{v_s} \frac{P_s^{-}(L)}{P_p^{\text{th}}} [G(z) - 1] \frac{G(L)}{G(z)} = 0, \qquad (21)$$

$$\ln G(z) = \gamma_e z + \beta \ln \left[\frac{P_p(z)}{P_p(0)} \right], \qquad (22)$$

Fig. 2 Signal fractional advancement as a function of z (forward-propagating signal, *solid lines*) or $L - z$ (backward-propagating signal, *dotted lines*): (**a**) the input pump power is not modulated; (**b**) the input pump power is modulated with a modulation index $r_p = 0.1$ and a phase $\varphi_p = \pi$
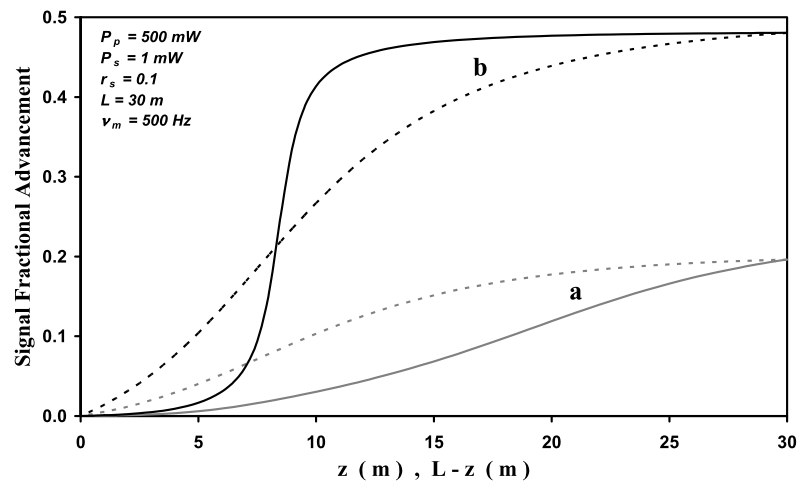
which are deduced [40] from Eqs. (1), (2), and (6), and where $G(z)$ is the gain at a point z of the EDF. $P_s^\pm(z)$ are related to $G(z)$ by means of

$$P_s^+(z) = P_s^+(0)G(z), \qquad P_s^-(z) = P_s^-(L)G(L)/G(z). \tag{23}$$

Considering Eqs. (20), (21), and (22) at $z = L$, it is verified that neither the amplifier gain nor the remaining pump power depends on the amplification scheme.

Finally, defining the threshold pump power as the pump power required to achieve amplification, we find by imposing the condition $G(L) = 1$ in Eqs. (20), (21), and (22) that the threshold pump power is given by

$$P_{\text{threshold}} = P_p^{\text{th}} \frac{\gamma_a}{\beta} L \left[1 - \exp\left(-\frac{\gamma_e}{\beta} L \right) \right]^{-1}. \tag{24}$$

This is a general result that does not depend on the amplification scheme. (By amplification scheme we mean whether the signal wave is forward or backward propagating.) For short lengths of fiber, this result shows that

$$P_{\text{threshold}} \approx P_p^{\text{th}} \frac{\gamma_a}{\gamma_e} \approx P_p^{\text{th}}, \tag{25}$$

but if the fiber length is long enough, we find that

$$P_{\text{threshold}} \approx P_p^{\text{th}} \frac{\gamma_a}{\beta} L, \tag{26}$$

and $P_{\text{threshold}}$ can be significantly greater that P_p^{th}. Nevertheless, P_p^{th} is a suitable approximation for the threshold power in many practical cases and this simplification is very useful, since P_p^{th} depends neither on the signal wavelength nor on the fiber length. Moreover, P_p^{th} is normally used as a reference power and pump powers are classified as weak or strong by a comparison with it.

Taking into account that the gain of the EDF does not depend on the amplification scheme, it seems reasonable to think that phases and modulation indexes are also independent of the amplification scheme. In fact, this property has been numerically verified for many cases. Although the signal phase and signal modulation index evolve along the fiber in different ways, their values at the ends of the EDF are equal for both amplification schemes. To illustrate this point, some examples are shown in Figs. 2 and 3. These numerical results have been computed assuming the following typical values for the EDF: $\gamma_p = 0.25$ m^{-1}, $\gamma_a = 0.4$ m^{-1}, $\gamma_e = 0.6$ m^{-1} ($\beta = 4$), $\tau = 10.5$ ms, and $P_p^{\text{th}} = 3.5$ mW. Furthermore, $\lambda_s = 1.55$ μm, $\lambda_p = 0.98$ μm, input pump power $= 500$ mW, input signal power $= 1$ mW, signal modulation index $= 0.1$, fiber length $= 30$ m, and modulation frequency $= 500$ Hz. In Fig. 2, the signal fractional advancement is graphed as a function of z (forward-propagating signal) or $L - z$ (backward-propagating signal) for two situations: (a) the input pump power is not modulated and (b) the input pump power is modulated with a modulation index $r_p = 0.1$ and a phase $\varphi_p = \pi$. In Fig. 3, the signal modulation index is shown as a function of z (forward-propagating signal) or $L - z$ (backward-propagating signal) for the situations: (a) the input pump power is not modulated and (b) the input pump power is modulated with a modulation index $r_p = 0.1$ and a phase $\varphi_p = \pi/2$. This lack of dependence on amplification scheme has been experimentally verified by employing a setup similar to that of Ref. [14].

Therefore, and considering that the phases and modulation indexes at the output of the EDF should be the most important predictions of our theoretical model, this study can be carried out working only with forward-propagating signal power, although then its evolution along z is lost. Thus, the superscript '$\pm$' can be suppressed, since henceforth a forward-propagating signal will be always assumed.

Fig. 3 Signal modulation index as a function of z (forward-propagating signal, *solid lines*) or $L - z$ (backward-propagating signal, *dotted lines*): (**a**) the input pump power is not modulated; (**b**) the input pump power is modulated with a modulation index $r_p = 0.1$ and a phase $\varphi_p = \pi/2$
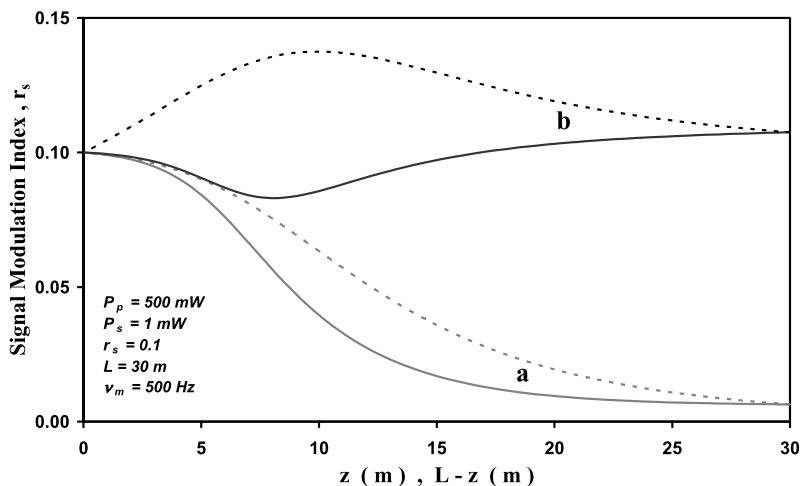
Substituting Eqs. (10) and (13) into Eqs. (15) and (19), and defining the parameters

$$\Delta\varphi_q(z) = \varphi_q(z) - \varphi_s(0), \quad q = s, p, \tag{27}$$

$$d_q(z) = r_q(z)/r_s(0), \quad q = s, p, \tag{28}$$

we find that the following coupled differential equations are obtained:

$$\frac{d}{dz}\Delta\varphi_s(z) = \frac{1}{\omega_c^2(z) + \omega_m^2}\left\{\frac{d\omega_c(z)}{dz}\omega_m - \frac{1}{d_s(z)}\frac{d\omega_p(z)}{dz}\right.$$
$$\left. \times\left[\omega_m\zeta_R(z) + \omega_c(z)\zeta_I(z)\right]\right\}, \tag{29}$$

$$\frac{d}{dz}d_s(z) = \frac{1}{\omega_c^2(z) + \omega_m^2}\left\{\frac{d\omega_p(z)}{dz}\left[\omega_c(z)\zeta_R(z) - \omega_m\zeta_I(z)\right]\right.$$
$$\left. - \frac{d\omega_c(z)}{dz}\omega_c(z)d_s(z)\right\}. \tag{30}$$

In these equations, we have defined

$$\zeta_R(z) = \cos\left[\Delta\varphi_s(z)\right]$$
$$- \beta d_p(0)\cos\left[\Delta\varphi_s(z) - \Delta\varphi_p(0)\right], \tag{31}$$

$$\zeta_I(z) = \sin\left[\Delta\varphi_s(z)\right]$$
$$- \beta d_p(0)\sin\left[\Delta\varphi_s(z) - \Delta\varphi_p(0)\right]. \tag{32}$$

By solving these equations at $z = L$, the delay/advancement of the signal power ($\Delta\varphi_s$) and the distortion of the signal power (d_s) can be quantified. It is necessary to point out that if there is no distortion, then $d_s = 1$ and, therefore, $d_s = 0$ dB. Moreover, this definition of the signal distortion assumes a sinusoidal input signal and would be equivalent to the amplitude response of the modulated signal power. However, if another kind of input signal is employed, it would be necessary to quantify signal distortion with other definitions, as in Ref. [35], where the authors analyze pulses as input signal considering broadening and pulse skew.

With $\Delta\varphi_s$ and d_s values, the additional parameters $\Delta\varphi_p$ (pump phase with regard to the phase of the coupled signal power) and d_p (pump modulation index with regard to the modulation index of the coupled signal power) can be also determined at $z = L$, taking into account that

$$d_p(L)\exp\left[i\Delta\varphi_p(L)\right]$$
$$= d_p(0)\exp\left[i\Delta\varphi_p(0)\right]$$
$$+ \frac{1}{\beta}\left\{d_s(L)\exp\left[i\Delta\varphi_s(L)\right] - 1\right\}. \tag{33}$$

To sum up, distortion and delay/advancement of the signal and pump powers can be computed as functions of L, $P_p(0)$, $P_s(0)$, $d_p(0)$, $\Delta\varphi_p(0)$, and ω_m by solving Eqs. (29), (30), and (33), together with Eqs. (1), (2), (6), (7), (18), (20), (22), (31), and (32). It is not necessary to take into account $\Delta\varphi_s(0)$ or $d_s(0)$, since $\Delta\varphi_s(0) = 0$ and $d_s(0) = 1$, by definition, and obviously, neither $r_s(0)$ nor $\varphi_s(0)$ influences the results.

In general, closed-form solutions cannot be found for the proposed model. Although the results shown in following sections are numerically obtained, analytic equations for some particular cases are also included.

3 Results for no modulation of the pump power

In spite of losing generality with regard to our proposed model, the case of using no modulation of the pump field is quite significant because experimental measurements have usually been reported for such a case. It is necessary to clarify that, even though the pump power injected at $z = 0$ is not modulated, the modulation of the signal induces a modulation of populations along the EDF and, therefore, of the pump power as well. In Fig. 4, the frequency dependence of the pump advancement/delay is shown for a signal power of 1 mW coupled into a 30-m-long EDF. The

Fig. 4 Frequency and pump power dependence of the pump fractional advancement/delay (with regard to the input signal modulation). Although the pump power coupled at $z = 0$ is not modulated, the modulation of the signal induces modulation of the pump power along the EDF. The pump power is advanced provided that it is higher than $P_{\text{threshold}} = 10.62$ mW (computed by Eq. (24))
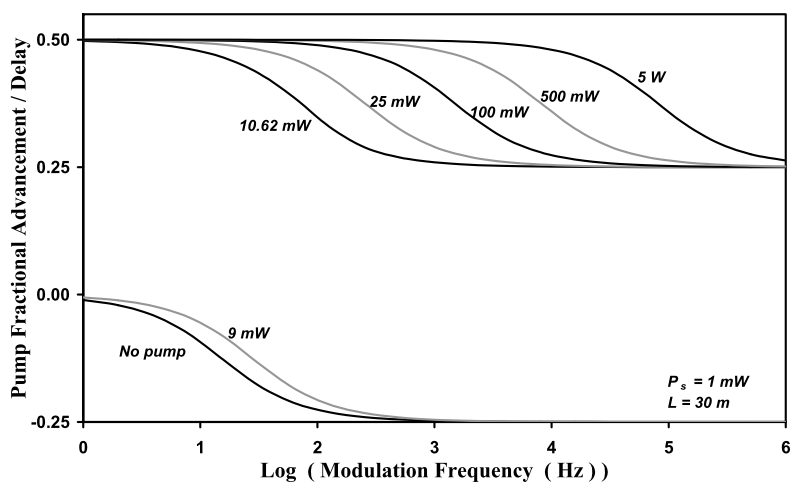
Fig. 5 Frequency and pump power dependence of the pump distortion. Although the pump power at $z = 0$ is not modulated, the modulation of the signal induces modulation of the pump power along the EDF
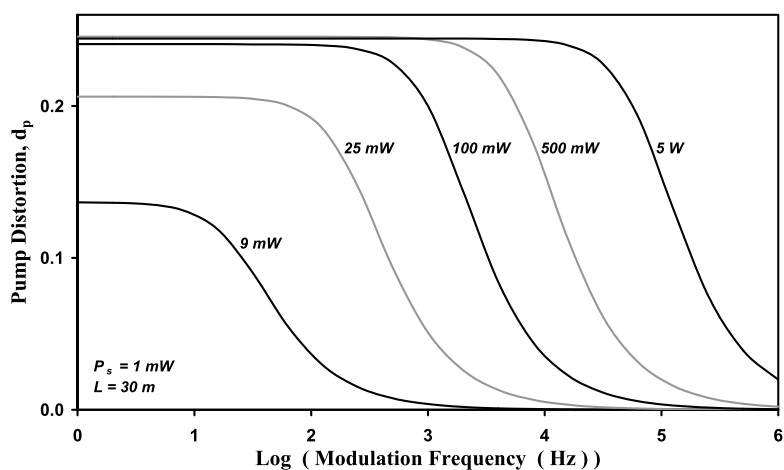
pump power is advanced provided that it is higher than $P_{\text{threshold}} = 10.62$ mW (computed by Eq. (24)). If the pump power is exactly $P_{\text{threshold}}$, then a step in the phase of the modulation of π radians is observed. As the modulation frequency is increased, fractional advancements vary from 0.5 (π) to 0.25 ($\pi/2$), while fractional delays vary from 0 to -0.25 ($-\pi/2$). Moreover, the frequency dependence of the pump distortion is shown in Fig. 5 for several pump powers. This modulation induced on the pump power has been also verified by measurement in a setup similar to the one of Ref. [14].

If no modulated pump power is coupled into the EDF, the main features of signal advancement/delay and signal distortion can be easily analyzed as a function of the modulation frequency, the pump power, and the EDF length, obtaining solutions in agreement with reported experimental results [14, 36, 37]. As it can be seen in Fig. 6, the sign of the signal phase variation does not depend on the frequency modulation ω_m. If the coupled pump power is exactly $P_{\text{threshold}}$ (defined by Eq. (24)), then $\Delta\varphi_s(L) = 0$, and neither advancements nor delays would be observed. This condition can be analytically deduced by imposing in Eqs. (29)–(32)

the condition that $d_s(z) = 1$ and $\Delta\varphi_s(z) = 0$ (that is to say, the signal power does not experiment any effect), and also that the coupled pump power is not modulated ($d_p(0) = 0$). Then, taking into account Eqs. (7) and (18), the condition $G(L) = 1$ should be accomplished and, in consequence, the coupled pump power should be exactly $P_{\text{threshold}}$. Thus, it is necessary to couple pump powers greater that this threshold value to obtain advancements of the signal power.

On the other hand, if $\omega_m \to \infty$ or $\omega_m \to 0$, then $\Delta\varphi_s \to 0$. Therefore, $\Delta\varphi_s$ must always have a maximum (for advancements) or a minimum (for delays) at some modulation frequency. As the pump power increases, this maximum/minimum shifts towards higher modulation frequencies, as can be clearly appreciated in Fig. 6. The greatest delays are obtained at low frequencies (25 Hz, if no pump is coupled) because the erbium lifetime is very long. However, the greatest advancements can be obtained at much higher frequencies (up to 15 kHz) provided that the input pump power is high enough. Moreover, the fractional advancement at the optimal frequency can be maximized by selecting the proper pump power for each length of the EDF.

Fig. 6 Frequency and pump power dependence of the signal fractional advancement/delay. The pump power coupled at $z = 0$ is not modulated. If the pump power is equal to $P_{\text{threshold}} = 10.62$ mW (computed by Eq. (24)), the signal phase does not change
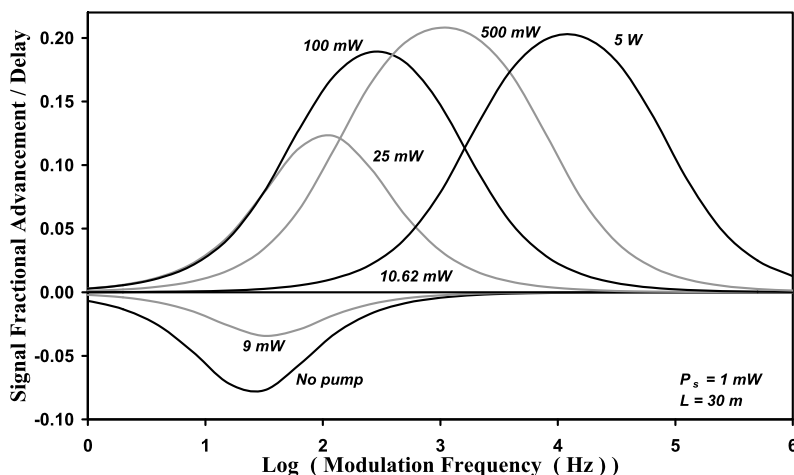
Fig. 7 Signal fractional advancement as a function of modulation frequency for several lengths of the EDF. The input pump power is not modulated
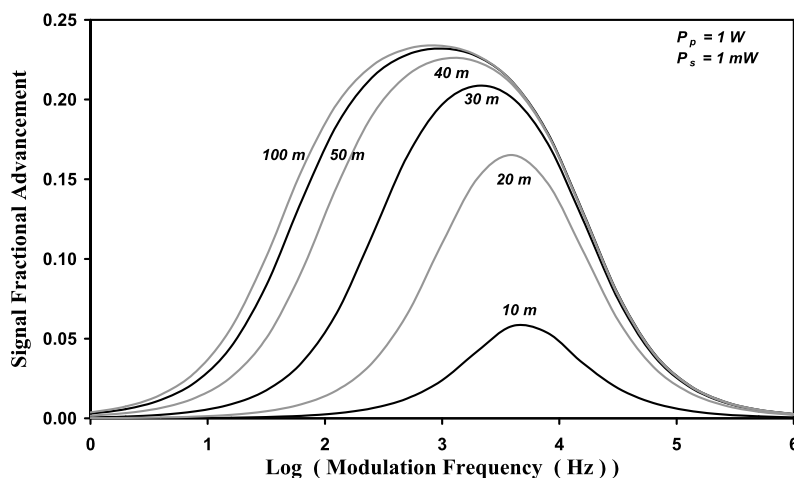
Fractional advancements of the signal are shown in Fig. 7 for several EDF lengths for 1 W pump power. Advancement values become greater as the length increases. Furthermore, a wider and flatter frequency response is observed. Unfortunately, its growth rate becomes slower as the length increases, and it is not worthwhile to use fibers longer than approximately 50 m. Moreover, it has been verified numerically that $\Delta\varphi_s$ always falls between $-\pi/2$ and $+\pi/2$, corresponding to fractional delays or advancements of 0.25. In fact, the limiting value of the fractional advancement (0.25) is practically obtained in Fig. 7. However, to obtain fractional delays near 0.25, it would be necessary to employ very long samples of unpumped EDF (hundreds of meters) and a high signal power (tens of mW), as can be seen in Fig. 8. If the signal power is high enough, greater delays are obtained for modulation frequencies around 200 Hz, which are quite higher than $1/\tau$ (typically 15 Hz).

This behavior of delays for an unpumped EDF can also be analytically demonstrated in this particular case since Eqs. (29) and (30) provide the following closed-form solu-

tions to $\Delta\varphi_s$ and d_s:

$$\Delta\varphi_s(L) = \arctan\left[\frac{\omega_c(L)}{\omega_m}\right] - \arctan\left[\frac{\omega_c(0)}{\omega_m}\right], \tag{34}$$

$$d_s(L) = \ln\sqrt{\frac{\omega_c^2(0) + \omega_m^2}{\omega_c^2(L) + \omega_m^2}}. \tag{35}$$

Taking into account that, if the EDF is unpumped, the signal power is always attenuated, and considering Eqs. (7) and (34), it is seen that there is a maximum phase variation given by

$$\Delta\varphi_{s,\text{max}} = \frac{\pi}{2} - 2\arctan\sqrt{\frac{\omega_c(0)}{\omega_c(L)}}, \tag{36}$$

at the modulation frequency

$$\omega_{\text{max}} = \sqrt{\omega_c(0)\omega_c(L)}. \tag{37}$$

As the signal power is attenuated, one finds that $\omega_c(0) \geq \omega_c(L)$, and therefore the signal delays cannot be greater than $\pi/2$.

Fig. 8 Signal fractional delays as a function of modulation frequency for several values of the input signal power. The EDF length is 200 m, except for the coupled signal power of 50 mW (the EDF length is 400 m)
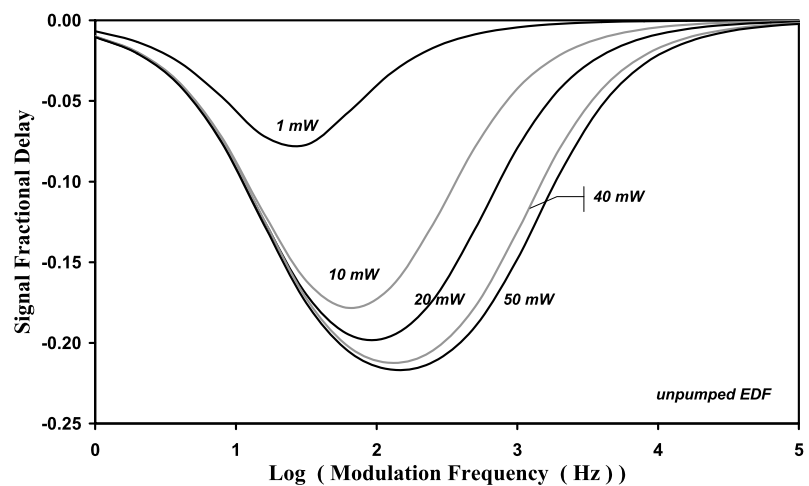
Fig. 9 Frequency and pump power dependences of the signal distortion. The pump power coupled at $z = 0$ is not modulated
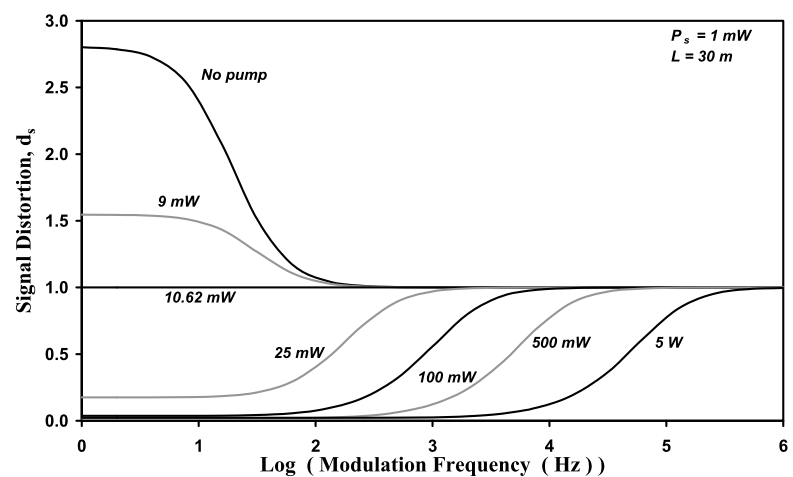
Although quite large advancements/delays of the signal power can be obtained by modulation at a suitable frequency, it is also necessary to analyze the signal distortion, which is as important as signal advancement/delay. In fact, advancing or delaying signal power is pointless if the output signal is excessively distorted.

The dependence of the distortion on the modulation frequency is shown in Fig. 9 for various pump powers. In this figure it is clearly seen that the signal could be so strongly distorted that it would be useless for any application, mainly for low frequencies, since d_s is much greater ($P_p < P_{\text{threshold}}$) or much lower ($P_p > P_{\text{threshold}}$) than unity. As the signal power is less distorted as the modulation frequency grows, it is necessary to modulate with high frequencies in order to reduce the signal distortion, although then signal advancements/delays are dramatically diminished.

As it is not possible to simultaneously maximize fractional advancements/delays while minimizing distortion, we must accept smaller fractional advancements/delays if we

require that distortion values be held below a suitable level. Thus, it is necessary to reach a compromise between these two requirements.

Thus, we should optimize the signal advancement by selecting a suitable pump power at each modulation frequency, but require always that distortion values be held lower than some maximum tolerable value. Taking into account the experimental results of Ref. [14], a distortion value lower than 2 dB can be estimated as tolerable. In this procedure, it is necessary to consider that the pump power is always limited to a realistic maximum value (currently, 10 W can be a suitable choice).

As an example, in Fig. 10, optimal fractional advancements are shown for several values of the available pump power, considering a 50-m-long EDF (in agreement with results of Fig. 7) and assuming distortion values lower than 1 dB. Up to some maximum frequency, the higher the modulation frequency, the greater the optimal fractional advancement, although the input pump power must be increased as well. From this maximum frequency, it would be necessary

Fig. 10 Maximum fractional advancement as a function of the modulation frequency always keeping distortion values lower than 1 dB and limiting the pump power to 30 mW, 300 mW, 10 W, 100 W, and 1 KW
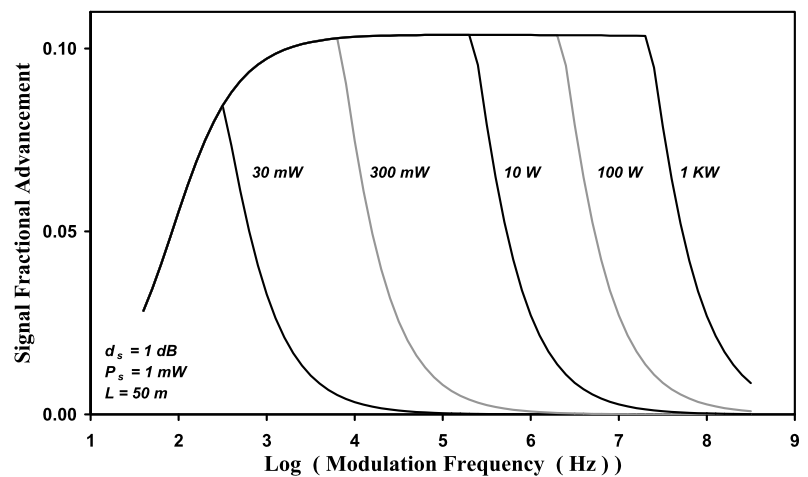
Fig. 11 Maximum fractional advancement as a function of the modulation frequency for different values of the allowable distortion ($d_s = 0.2, 0.5, 1, 2,$ and 3 dB) and imposing a limited pump power (100 W)
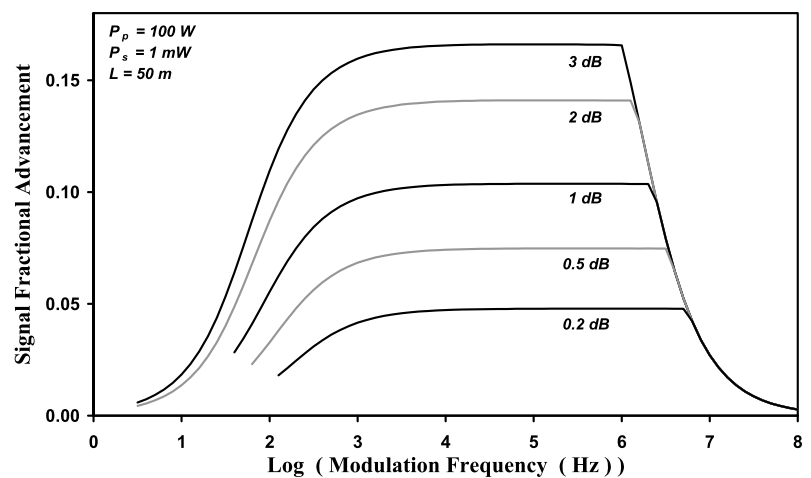
to inject a pump power greater than 10 W, but this is not possible because the available pump power is limited and in consequence the optimized advancement is diminished. If the available pump power were 10 W, fractional advancements slightly greater than 0.1 would be obtained from 2 to 200 kHz, with a very flat frequency response. If the available pump power were much higher (1 KW), this frequency range could be increased up to 25 MHz. The frequency response would be very flat, although fractional advancements would not be improved. To obtain significant signal advancements at higher frequencies, the input pump power required would be enormous. Were such a high pump power actually used, we would have to generalize this theoretical model in order to include other nonlinear effects.

Of course, maximum fractional advancements can be larger if we permit a greater amount of signal distortion, as is shown in Fig. 11. Thus, fractional advancements grow up to 0.14 and 0.17 for allowable distortion values of 2 and 3 dB, respectively. Nevertheless, although frequency responses are always very flat, frequency ranges are slightly narrower as distortion values are increased: 5, 2 and 1 MHz for 0.2, 1 and 3 dB, respectively.

## 4 Enhanced results by modulating the pump power

In the last paragraph a method that enhances the frequency response of EDF has been discussed, although advancements and delays are limited to quite low values. Nevertheless, it is possible to enhance results by modulating the pump power. In fact, as it is shown in Figs. 12 and 13, by modifying the pump phase (with regard to the signal phase) around $\Delta\varphi_p = \pi$, the signal power can be advanced or delayed, reaching fractional advancements/delays near 0.5 along a wide and flat range of modulation frequencies. Logically, this frequency range depends on the coupled pump power and the EDF length. Besides, this pump phase is the most suitable since the signal power is not distorted (see Fig. 13). Therefore, it seems clear that this method offers two very important advantages for future applications: as slow and fast light can be obtained in an amplified signal (slow light and absorption are not necessarily associated), and the signal power is weakly distorted.

As can be seen in Fig. 12, this frequency range is limited by a well-defined modulation frequency where an abrupt change from delays to advancements appears for some pump

Fig. 12 Signal fractional advancement/delay as a function of modulation frequency for several values of the phase of the modulation of the pump. Both powers have the same modulation index ($d_p = 1$)
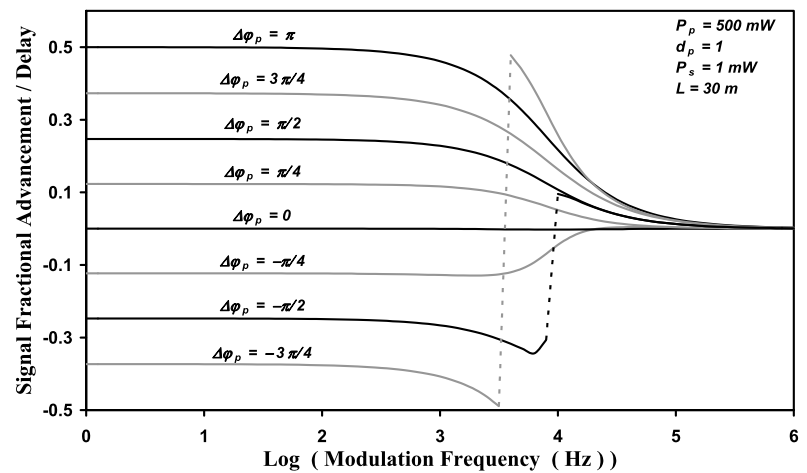
Fig. 13 Signal distortion as a function of modulation frequency for several different values of the phase of the pump modulation. Both powers have the same modulation index ($d_p = 1$)
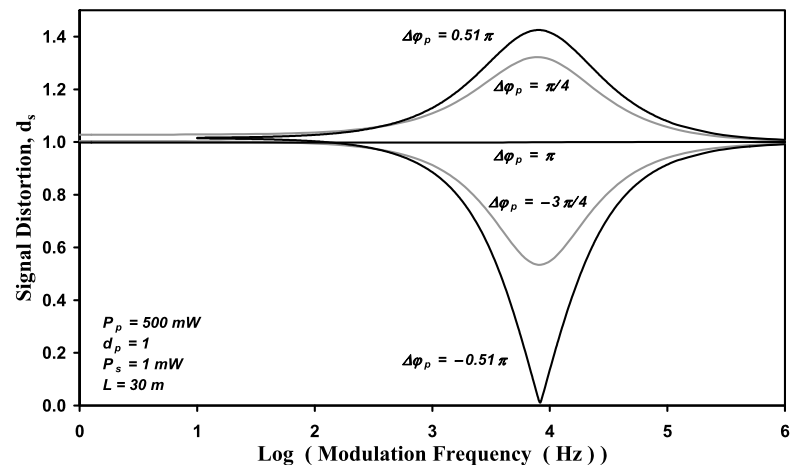
phase values. This modulation frequency depends on the coupled pump power, on the EDF length, and the pump phase.

If the EDF sample is too short, fractional advancements/delays always are lower, although it is possible to advance or delay the signal power by modifying the pump phase, as it can be seen in Fig. 14. However, if the sample is long enough, this transition becomes a sharp change for pump phases near π. In fact, the value of the pump phase approaches π as the EDF length is increased.

In order to verify that this sudden transition is not a mathematical trick, its evolution under slight changes of the pump phase is analyzed. As shown in Fig. 15, although the transition from delays to advancements as a function of the modulation frequency can be smooth, it can be made progressively sharper by slight changes of the pump phase until it turns into a discontinuity. In this case, the discontinuity is produced at a well-defined modulation frequency ($\nu_d = 8.138$ kHz) by a pump phase of -0.51π, and there is a 2π change in the signal phase. This modulation frequency matches up with the value of $\omega_c(L)/(2\pi)$. This result has been numerically checked for other pump powers (200 mW,

500 mW, 1 W and 5 W) and lengths (20, 30 and 50 m). Moreover, the discontinuity always appears for the pump phases from -0.51π to $-\pi$.

This interesting behavior is worthy of a more detailed analysis to understand its main causes. It is difficult to explain since populations are modulated by the pump power and the amplified signal power, and this modulation also influences the dynamics of both powers. Nevertheless, the explanation should be related to the amplitude responses of the signal power and the ground level. The modulation index, $r_n(z)$, and the phase of the ground-level population, $\varphi_n(z)$, can be determined by differentiating Eq. (13) with regard to z and taking into account Eqs. (10) and (12). As can be appreciated in Fig. 13, the amplitude response of the output signal power changes only if the modulation frequency is around ν_d. If the pump phase is positive, then this response is greater than unity. However, if the pump phase is negative, it is lower than unity and it is even zero at ν_d if $\Delta\varphi_p(0) = -0.51\pi$. The amplitude response of the ground level population as a function of the modulation frequency is displayed in Fig. 16 for several values of the pump phase. This response does not depend on the sign of

Fig. 14 Signal fractional advancement/delay as a function of the phase of the pump modulation for several different values of the EDF length
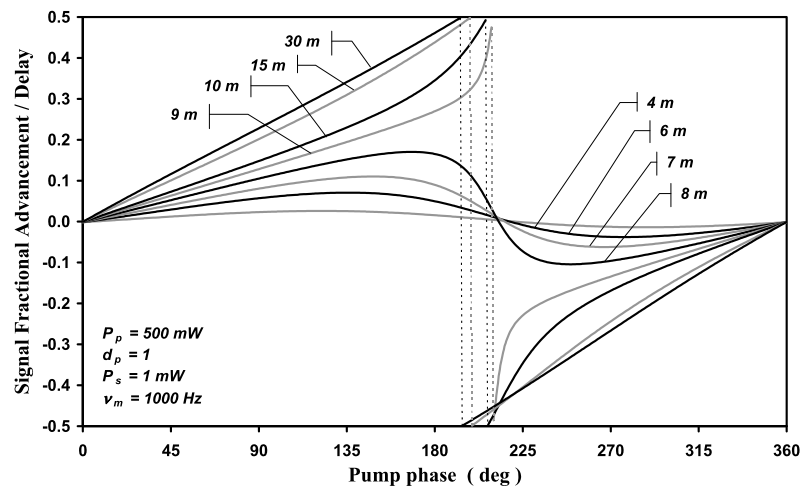
Fig. 15 Transition from delayed to advanced signal for several pump phases around -0.5π. $\Delta\varphi_p = -0.51\pi$ (*circles*), -0.504π (*triangles*), -0.5π (*squares*), and -0.45π (*diamonds*)
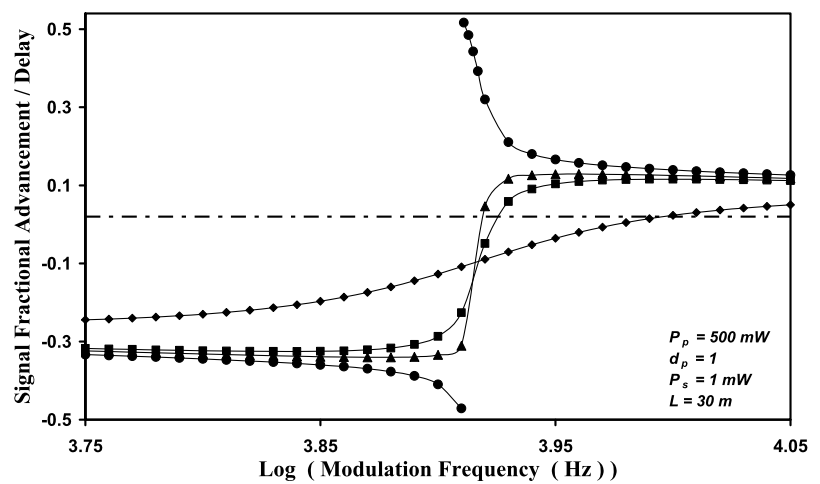
Fig. 16 Modulation index of the ground-level population as a function of the modulation frequency for several values of the pump modulation phase. Note that the results do not depend on the sign of the pump phase. Its minimum and maximum values are always found if the pump phase is 0 or π, respectively, and it has always a maximum for modulation frequencies around ν_d
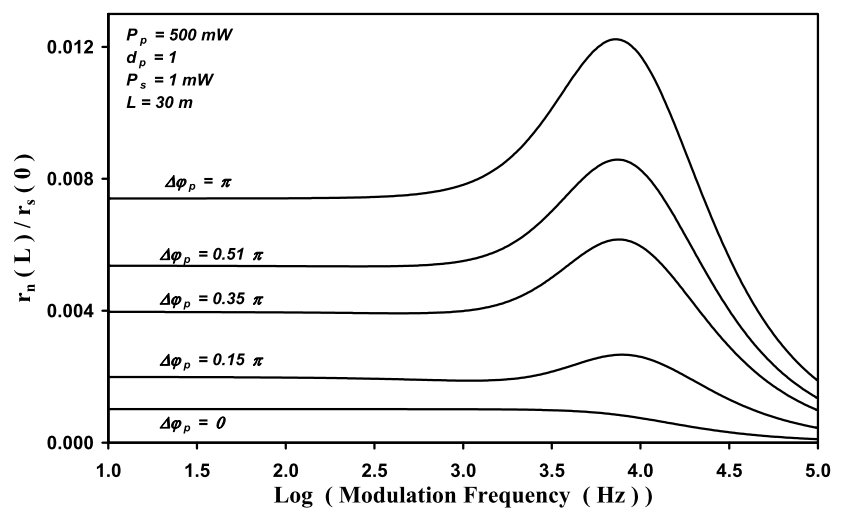
the pump phase. Its minimum and maximum values are always found if the pump phase is 0 or π, respectively, and it has always a maximum (like a resonance) for modulation frequencies around ν_d. In order to complete this analysis, both responses and the output signal advancement/delay as functions of the input pump phase can be seen in Figs. 17 and 18 for three significant modulation frequencies: 10 Hz (very low frequency), 8.3 kHz (slightly greater than ν_d) and

Fig. 17 Dependence of the
signal distortion (*black lines*)
and of the modulation index of
the ground-level population
(*gray lines*) on the phase of the
pump intensity modulation for
three significant modulation
frequencies. The pump phase of
-0.51π is marked because the
discontinuity of the signal
advancement/delay is found for
pump phases from -0.51π to
$-\pi$
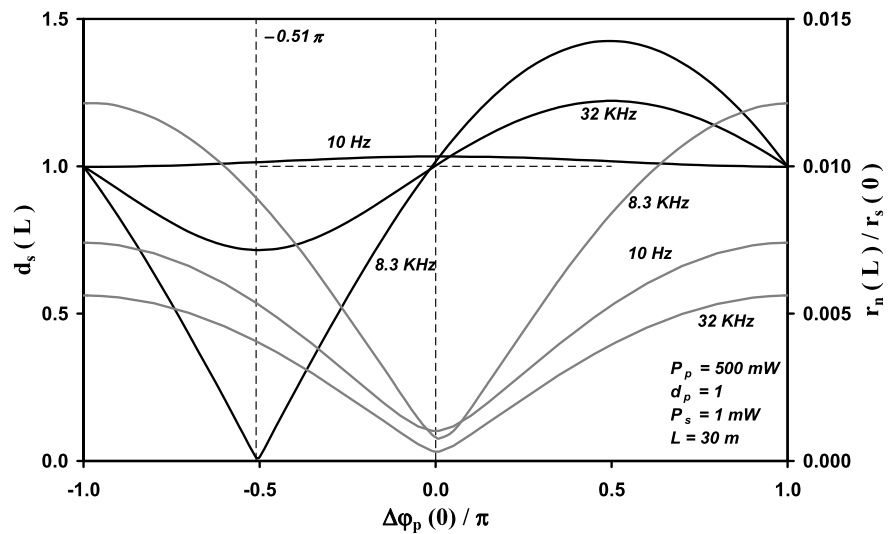
Fig. 18 Dependence of the
signal advancement/delay on the
phase of the pump modulation
for the three modulation
frequencies considered in
Fig. 17
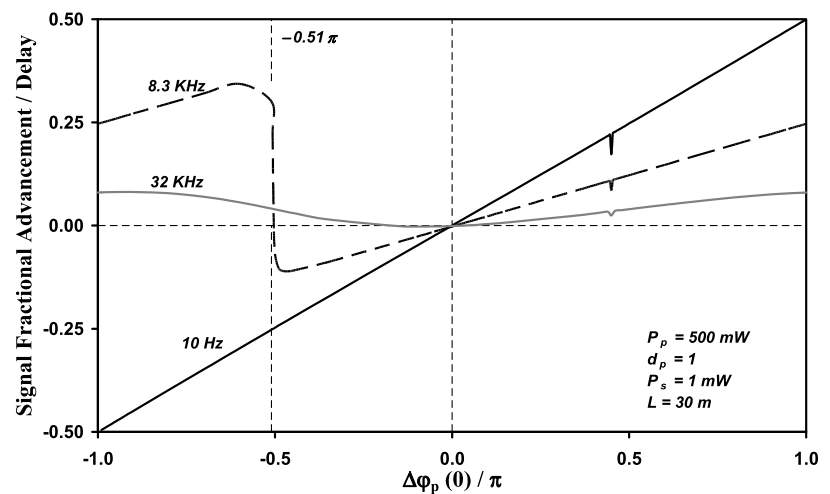
32 kHz (much greater than ν_d). Modulating at low frequencies (10 Hz), the amplitude response of the signal has a parabolic profile, which is maximum at $\Delta\varphi_p(0) = 0$ and minimum at $\Delta\varphi_p(0) = \pm\pi$. If $\Delta\varphi_p(0) = 0$, the population response is minimum and then the signal advancement/delay is always zero. Besides, the signal advancement/delay is linearly growing with regard to the pump phase. Apparently, if the modulation frequency is near ν_d, the signal response and the signal advancement/delay seem to strongly change their behavior. However, taking into account that both functions are periodic, it can be seen that their behavior is not so different. In Figs. 17 and 18, it would be sufficient to show both functions for a 2π-period from -0.5π to 1.5π to verify that the signal advancement/delay is linearly growing with regard to the pump phase and the response signal has again a shifted parabolic profile, reaching its maximum value for a pump phase of 0.5π, and its values vary in a much wider range, from 0 to 1.4. Therefore, as the modulation frequency increases, the discontinuity of the signal

advancement/delay is shifted to higher values of the pump phase, from $-\pi$ to -0.51π. However, if the modulation frequency is much greater than ν_d, the amplitude response of the energy-level population decreases fast and a clear change is produced. The signal response is again a parabola (maximum value at 0.5π) provided that the pump phase is positive, but it becomes an inverted parabola (minimum value at -0.51π) if the pump phase is negative. Then, the signal advancement/delay is always positive and it gives up being a linearly growing function. Finally, it is interesting to point out that the signal advancement/delay always presents a slight deviation of the linear growing (a shallow hole) at 0.45π, near the maximum of the amplitude response of the signal power.

In Figs. 12–18, the condition $d_p(0) = 1$ is always imposed. Taking into account the behavior shown in Figs. 19 and 20, it seems quite clear that pump and signal powers should have the same modulation index ($d_p(0) = 1$), in order to enhance the frequency response for signal advance-

Fig. 19 Signal fractional advancement as a function of modulation frequency for several different pump modulation indexes. The pump phase at $z = 0$ is $\Delta \varphi_p = \pi$
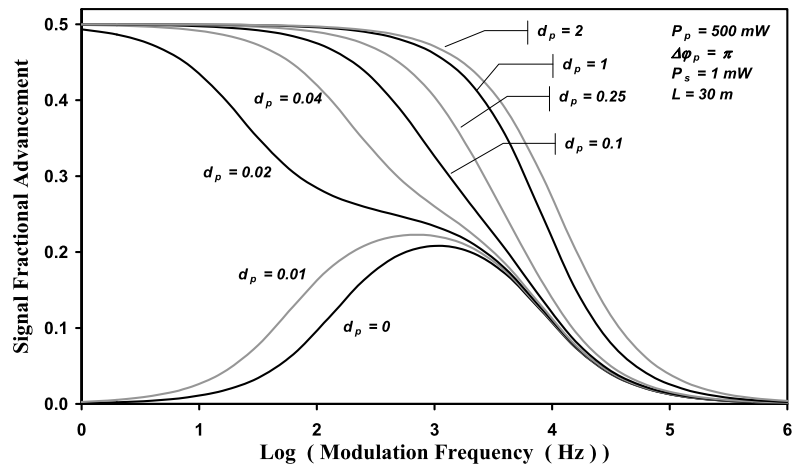
Fig. 20 Distortion of the signal as a function of modulation frequency for several different modulation indexes of the pump. The phase of the pump modulation at $z = 0$ is $\Delta \varphi_p = \pi$
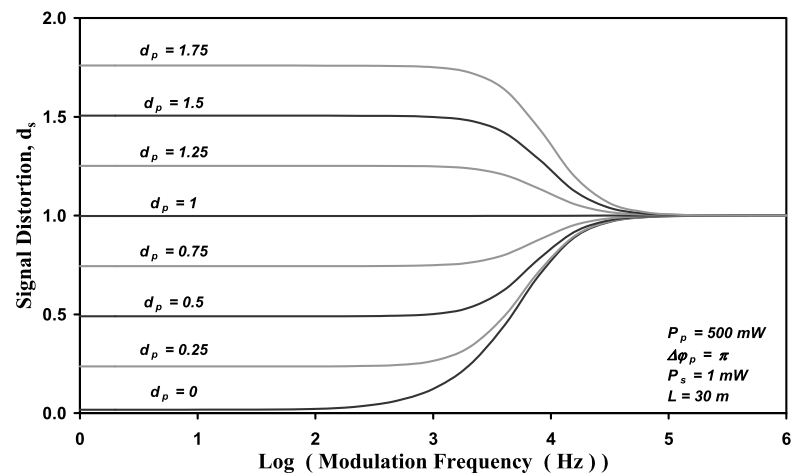
ments/delays and to ensure that the signal power is not affected by distortion.

On the other hand, in order to analyze how the pump power influences the modulation frequency where the transition from delays to advancements is obtained, the condition $d_s(z) \approx 1$ must be imposed on Eqs. (29) and (30). Then,

$$\frac{d}{dz} \Delta \varphi_s(z) = \frac{d\omega_c(z)}{dz} \frac{\zeta_I(z)}{\omega_m \zeta_I(z) - \omega_c(z)\zeta_R(z)}, \qquad (38)$$

and taking into account that Eqs. (31) and (32) can be rewritten as

$$\frac{d\zeta_R(z)}{dz} = -\zeta_I(z) \frac{d}{dz} \Delta \varphi_s(z), \qquad (39)$$

$$\frac{d\zeta_I(z)}{dz} = \zeta_R(z) \frac{d}{dz} \Delta \varphi_s(z), \qquad (40)$$

then Eq. (38) can be expressed as

$$\frac{d}{dz} \left[\omega_m \zeta_R(z) + \omega_c(z)\zeta_I(z) \right] = 0. \qquad (41)$$

By integrating this equation from $z = 0$ to $z = L$ and substituting again Eqs. (31) and (32), it is obtained that

$$\begin{aligned} \Big\{ \big[\omega_m \zeta_R(0) + \omega_c(L)\zeta_I(0) \big] \tan\big[\Delta \varphi_s(L)/2\big] \\ + \omega_m \zeta_I(0) - \omega_c(L)\zeta_R(0) \Big\} \sin\big[\Delta \varphi_s(L)\big] \\ = \big[\omega_c(L) - \omega_c(0)\big]\zeta_I(0), \end{aligned} \qquad (42)$$
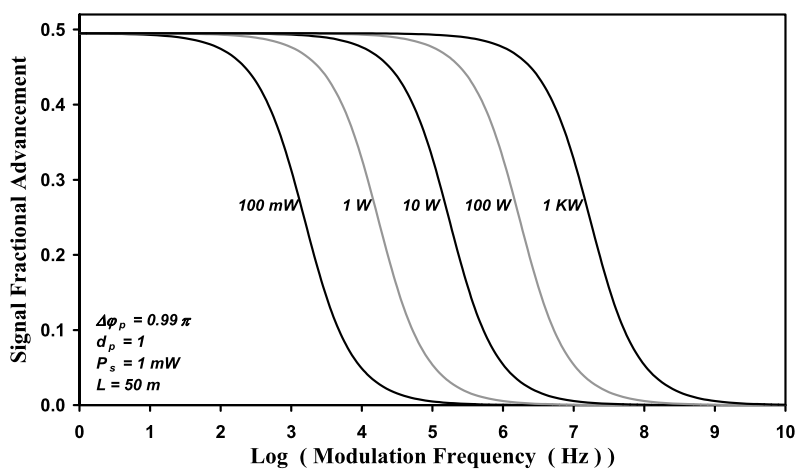
with

$$\begin{aligned} \zeta_I(0) &= \beta d_p(0) \sin\big[\Delta \varphi_p(0)\big], \\ \zeta_R(0) &= 1 - \beta d_p(0) \cos\big[\Delta \varphi_p(0)\big]. \end{aligned} \qquad (43)$$
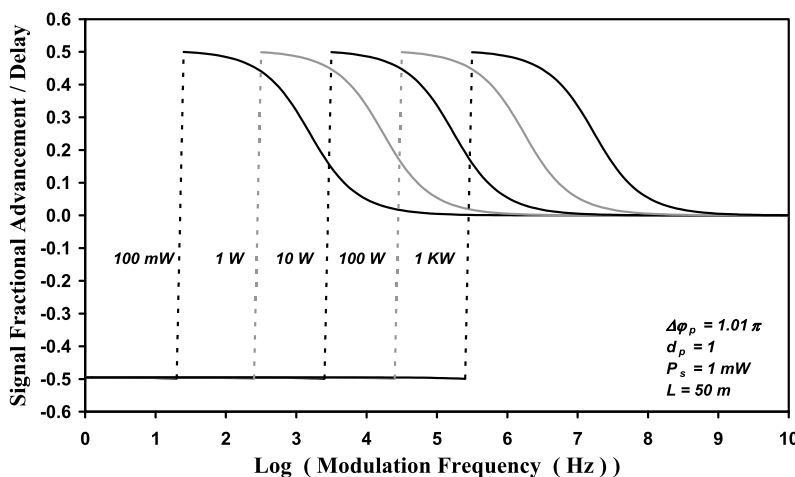
If $\Delta \varphi_p(0) = \pi$, the following solution is found for Eq. (42):

$$\Delta \varphi_s(L) = \pi - 2 \arctan\left[\frac{\omega_m}{\omega_c(L)}\right]. \qquad (44)$$

Fig. 21 Signal fractional
advancement as a function of
modulation frequency for
several different pump powers.
The pump phase at $z = 0$ is
$\Delta\varphi_p = 0.99\pi$

Fig. 22 Signal fractional
advancement/delay as a function
of modulation frequency for
several values of the pump
powers. The phase of the pump
modulation at $z = 0$ is
$\Delta\varphi_p = 1.01\pi$

Considering now that $d_p(0) = 1$ and $\Delta\varphi_p(0) = (1 + \varepsilon)\pi$ (with $|\varepsilon| \ll 1$), Eq. (42) can be approximately solved as

$$\Delta\varphi_s(L) = -\pi - 2\arctan\left[\frac{\omega_m}{\omega_c(L)} - \frac{\beta}{1+\beta}\varepsilon\pi\right],$$

$$\text{if } \frac{\omega_m}{\omega_c(L)} < \frac{\varepsilon\pi\beta}{1+\beta}, \quad \text{and} \tag{45}$$

$$\Delta\varphi_s(L) = \pi - 2\arctan\left[\frac{\omega_m}{\omega_c(L)} - \frac{\beta}{1+\beta}\varepsilon\pi\right],$$

otherwise.

Thus, if the pump phase is slightly lower than π ($\varepsilon \leq 0$), then the signal power is advanced. Otherwise, it will be delayed if the pump phase is slightly higher than π ($\varepsilon > 0$).

On the other hand, the range of modulation frequencies where advancements/delays are near 0.5 depends mainly on the coupled pump power and the EDF length, since these parameters have influence on $\omega_c(L)$. Basically, the higher $\omega_c(L)$, the wider the range of frequencies. As $\omega_c(L)$ increases as the coupled pump power is raised, the range of frequencies can be widened by coupling very high pump

powers. This behavior can be clearly appreciated in Figs. 21 and 22. Equations (29)–(32) have been solved for 50-m-long EDF. If the pump phase at $z = 0$ is $\Delta\varphi_p = 0.99\pi$ (see Fig. 21), then the frequency response is kept rather flat up to quite high modulation frequencies, since signal fractional advancements exceed 0.4 up to 50 kHz for a pump power of 10 W. This frequency modulation could be increased up to 5 MHz by coupling a pump power as high as 1 KW. If $\Delta\varphi_p = 1.01\pi$ (see Fig. 22), then the signal power is delayed with a totally flat frequency response up to 2.5 kHz for a pump power of 10 W. This frequency modulation could be increased up to 250 kHz by coupling a pump power as high as 1 KW. Signal fractional delays are practically 0.5 along these ranges. Unfortunately, the signal power is always advanced by EDF when it is modulated to higher frequencies.

Furthermore, the signal power will be very slightly distorted, provided that the pump power is high enough. Thus, whether $\Delta\varphi_p = 0.99\pi$ or $\Delta\varphi_p = 1.01\pi$, by coupling pump powers greater than 1 W, signal distortion values are always lower than 0.1 dB. Even if the pump power is 500 mW, signal distortion values are lower than 0.2 dB. But if the pump is only 100 mW, distortion can reach values as great as

Fig. 23 Comparison of the approximate results of Eq. (45) (*lines*) with the numerical results of Eqs. (29)–(32) (*symbols*)
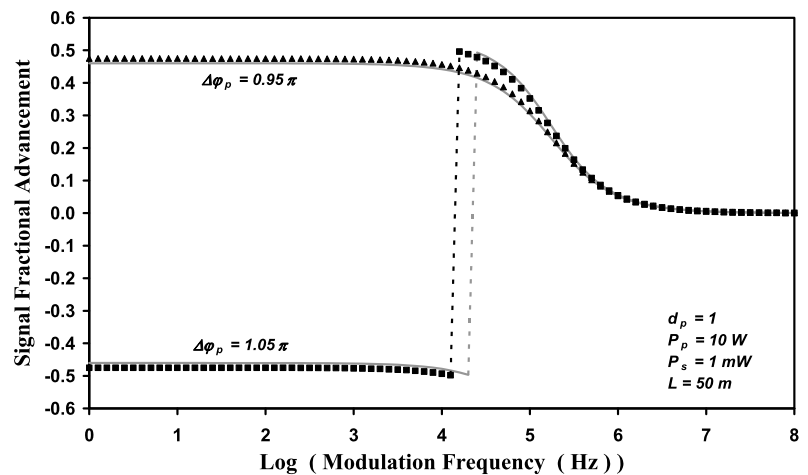
0.8 dB. Therefore, to apply these results, the lowest suitable pump power would be around 500 mW.

By comparison between Figs. 11 and 21, it is clear that this procedure based on the control of the pump phase enhances dramatically the frequency response. For instance, in Fig. 11, signal fractional advancements are never greater that 0.05 if the signal distortion is kept below 0.2 dB, although its frequency response is flat up to 5 MHz. However, in Fig. 21, the signal fractional advancement is much greater for every frequency since, even at 5 MHz, it has only decayed to 0.1.

Signal fractional advancements/delays have been computed by solving Eqs. (29)–(32) and by Eq. (45) as well, in order to check this approximation. Some representative results are shown in Fig. 23 for $\Delta\varphi_p = 0.95\pi$ and for $\Delta\varphi_p = 1.05\pi$. While pump powers higher than 500 mW are used, relative errors that affect advancements/delays are always lower than 4 %. However, for $\Delta\varphi_p = 1.05\pi$, the modulation frequency where delayed signal changes abruptly to advanced signal is not accurately determined by Eq. (45). In Fig. 23, this inaccuracy is not appreciable since the relative error that affects its logarithm is quite lower (around 5 %).

Finally, it is worth pointing out that these theoretical predictions are in agreement with the experimental demonstration reported in Ref. [38], as can be seen by comparing our Fig. 14 with Fig. 3 of Ref. [38], and our Figs. 12 and 21 with Fig. 4 of Ref. [38]. Unfortunately, this qualitative comparison cannot be made quantitative, because in Ref. [38] the results are obtained using low pump powers and short lengths.

5 Conclusions

By using the theoretical model presented here, it is possible to obtain advancements, delays, and distortion values as a function of the modulation frequency, the input pump power, modulation indexes of pump and signal powers, the input signal power, the fiber length, and the pump phase with respect to the signal phase. Predicted values do not depend on the direction of propagation of the signal power (forward or backward propagating).

Although the pump power is not modulated, advancements can be optimized such that distortion values remain tolerable by varying the input pump power at each modulation frequency. This procedure provides a quite flat frequency response up to kHz-range, although advancements are limited to low values. This flat response could be extended up to MHz-range provided that enormous pump powers were available. Nevertheless, advancement values would not be improved.

By modulating the pump power and controlling the phase of the modulation, the signal power can be delayed or advanced, and advancements and delays are dramatically enhanced. Thus, fractional advancements/delays near 0.5 are obtained with very low distortion varying the pump phase around π with regard to the signal phase. Moreover, the frequency response is not made worse for advancements and it is improved for delays (up to kHz-range). Finally, this method breaks the relationships of delayed signal and absorption and of advanced signal and gain, which could be essential for future applications based on slow and fast light.

Although these results have been computed considering a particular EDF, they can be easily extrapolated to other similar EDFs, provided that other nonlinear effects such as quenching and up-conversion can be neglected, since it can be assumed that neither the lifetime nor cross sections change. In order to compare results for different fibers, it is necessary only to consider the following three parameters: $P_p(0)/P_p^{\text{th}}$, $P_s^{\pm}(0)/P_p^{\text{th}}$ and $N_T L$ (N_T being the concentration of erbium-ions), since γ_p, γ_a, and γ_e are proportional to N_T. For example, if N_T were to be multiplied by two, we would have to divide the fiber length by two to obtain the previous results, since P_p^{th} does not depend on N_T.

Finally, this theoretical model could be easily modified to treat other types of optical amplifiers such as semiconductor

optical amplifiers. Although modulation frequencies would be shifted to GHz-range because their lifetime is much shorter (typically nanoseconds), their behavior should not offer great changes, provided that the amplifier was strongly pumped.

References

1. D. Budker, D.F. Kimball, S.M. Rochester, V.V. Yashchuck, Phys. Rev. Lett. **83**, 1767 (1999)
2. L.V. Hau, S.E. Harris, Z. Dutton, C.H. Behroozi, Nature **397**, 594 (1999)
3. M.S. Bigelow, N.N. Lepeshkin, R.W. Boyd, Phys. Rev. Lett. **90**, 113903 (2003)
4. M.S. Bigelow, N.N. Lepeshkin, R.W. Boyd, Science **301**, 200 (2003)
5. Y. Okawachi, M.S. Bigelow, J.E. Sharping, Z.M. Zhu, A. Schweinsberg, D.J. Gauthier, R.W. Boyd, A.L. Gaeta, Phys. Rev. Lett. **94**, 153902 (2005)
6. K.Y. Song, M. González-Herráez, L. Thévenaz, Opt. Express **13**, 82 (2005)
7. M. González-Herráez, K.Y. Song, L. Thévenaz, Appl. Phys. Lett. **87**, 081113 (2005)
8. J.E. Sharping, Y. Okawachi, A.L. Gaeta, Opt. Express **13**, 6092 (2005)
9. X. Zhao, P. Palinginis, B. Pesala, C.J. Chang-Hasnain, P. Hemmer, Opt. Express **13**, 7899 (2005)
10. E. Baldit, K. Bencheikh, P. Monnier, J.A. Levenson, V. Rouget, Phys. Rev. Lett. **95**, 143601 (2005)
11. M. González Herráez, K.Y. Song, L. Thévenaz, Opt. Express **14**, 1395 (2006)
12. H. Su, S.L. Chuang, Appl. Phys. Lett. **88**, 061102 (2006)
13. B. Pesala, Z. Chen, A.V. Uskov, C. Chang-Hasnain, Opt. Express **14**, 12968 (2006)
14. A. Schweinsberg, N.N. Lepeshkin, M.S. Bigelow, R.W. Boyd, S. Jarabo, Europhys. Lett. **73**, 218 (2006)
15. A. Lezama, A.M. Akulshin, A.I. Sidorov, P. Hannaford, Phys. Rev. A **73**, 033806 (2006)
16. Z. Lu, Y. Dong, Q. Li, Opt. Express **15**, 1871 (2007)
17. Z.C. Zhuo, B.S. Ham, Eur. Phys. J. D **49**, 117 (2008)
18. Y. Zhao, H.W. Zhao, X.Y. Zhang, B. Yuan, S. Zhang, Opt. Laser Technol. **41**, 517 (2009)
19. B. Pesala, F. Sedgwick, A.V. Uskov, C. Chang-Hasnain, Opt. Express **17**, 2188 (2009)
20. R.S. Tucker, P.C. Ku, C.J. Chang-Hasnain, J. Lightwave Technol. **23**, 4046 (2005)
21. E. Shumakher, N. Orbach, A. Nevet, D. Dahan, G. Eisenstein, Opt. Express **14**, 5877 (2006)
22. S.J.B. Yoo, J. Lightwave Technol. **24**, 4468 (2006)
23. R.S. Tucker, J. Lightwave Technol. **24**, 4655 (2006)
24. B. Zhang, L. Yan, I. Fazal, L. Zhang, A.E. Willner, Z. Zhu, D.J. Gauthier, Opt. Express **15**, 1878 (2007)
25. A. Zadok, O. Raz, A. Eyal, M. Tur, IEEE Photonics Technol. Lett. **19**, 462 (2007)
26. P.C. Ku, C.J. Chang-Hasnain, S.L. Chuang, J. Phys. D, Appl. Phys. **40**, R93 (2007)
27. L. Xing, L. Zhan, S. Luo, Y. Xia, IEEE J. Quantum Electron. **44**, 1133 (2008)
28. R.M. Camacho, C.J. Broadbent, I. Ali-Khan, J.C. Howell, Phys. Rev. Lett. **98**, 043902 (2007)
29. Z. Shi, R.W. Boyd, D.J. Gauthier, C.C. Dudley, Opt. Lett. **32**, 915 (2007)
30. Z. Shi, R.W. Boyd, Phys. Rev. Lett. **99**, 240801 (2007)
31. J. Freeman, J. Conradi, IEEE Photonics Technol. Lett. **5**, 224 (1993)
32. S. Jarabo, J. Opt. Soc. Am. B **14**, 1846 (1997)
33. S. Novak, A. Moesle, J. Lightwave Technol. **20**, 975 (2002)
34. G.M. Gehring, A. Schweinsberg, C. Barsi, N. Kostinski, R.W. Boyd, Science **312**, 895 (2006)
35. H. Shin, A. Schweinsberg, G. Gehring, K. Schwertz, H.J. Chang, R.W. Boyd, Q.H. Park, D.J. Gauthier, Opt. Lett. **32**, 906 (2007)
36. S. Melle, O.G. Calderón, F. Carreño, E. Cabrera, M.A. Antón, S. Jarabo, Opt. Commun. **279**, 53 (2007)
37. W. Qiu, Y.D. Zhang, J.B. Ye, N. Wang, J.F. Wang, H. Tian, P. Yuan, Chin. Phys. Lett. **25**, 489 (2008)
38. F. Arrieta-Yañez, S. Melle, O.G. Calderón, M.A. Antón, F. Carreño, Phys. Rev. A **80**, 011804(R) (2009)
39. H. Shin, A. Schweinsberg, R.W. Boyd, Opt. Commun. **282**, 2085 (2009)
40. S. Jarabo, M.A. Rebolledo, Appl. Opt. **34**, 6158 (1995)
41. S. Jarabo, J.M. Álvarez, Appl. Opt. **35**, 4759 (1996)
42. S. Jarabo, I.J. Sola, J. Sáez-Landete, J. Opt. Soc. Am. B **20**, 1204 (2003)